Behavior of three-dimensional subassemblages

Autor(en): **Morino, S. / Kawaguchi, J. / Uchida, Y.**

Objekttyp: **Article**

Zeitschrift: **IABSE reports = Rapports AIPC = IVBH Berichte**

Band (Jahr): **60 (1990)**

PDF erstellt am: **23.07.2024**

Persistenter Link: https://doi.org/10.5169/seals-46483

Behavior of Three-Dimensional Subassemblages

Comportement de sous-assemblages tridimensionnels

Das Verhalten von dreidimensionalen Stahlbetonrahmen

S. MORINO
Professor
Mie Univ.
Tsu, Japan

J. KAWAGUCHI
Assistant
Mie Univ.
Tsu, Japan

Y. UCHIDA
Associate Professor
Kagoshima Univ.
Kagoshima, Japan

C. YASUZAKI
Graduate Student
Mie Univ.
Tsu, Japan

1. OBJECTIVES

Beam-and-column subassemblage in a multi-story frame under the earthquake is subjected to the repeated flexure with shear about one axis, in addition to the constant vertical load and the constant flexure about the other axis. The objectives of the research presented here are to investigate the overall elasto-plastic behavior of the steel reinforced concrete (SRC) beam-and-column sub-assemblage subjected to the column axial thrust and the bi-directional beam loads, and clarify the effect of the three-dimensional loading on the maximum strength, deformation capacity and energy dissipation capacity.

2. EXPERIMENTAL INVESTIGATION

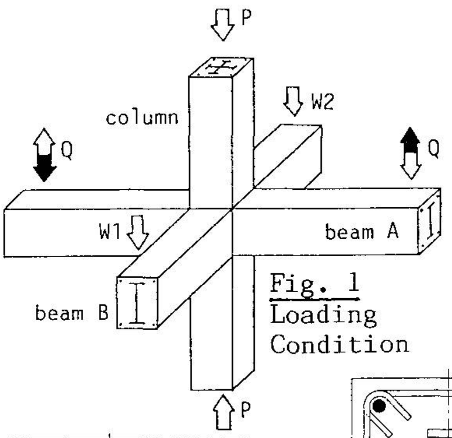

Fig. 1 Loading Condition

Figure 1 is the schematical illustration of a specimen and loading condition. The specimen is subjected to a constant axial thrust P on the column, and constant vertical long-term loads W_1 and W_2 at the tips of short beams (beam B). A couple of anti-symmetrical vertical loads Q are repeatedly applied at the tips of long beams (beam A), simulating the earthquake load. Table 1 shows the experimental parameters: failure type (column- or panel-failing type); pattern of the short-beam loads (equal or unequal); and intensity of the axial thrust P.

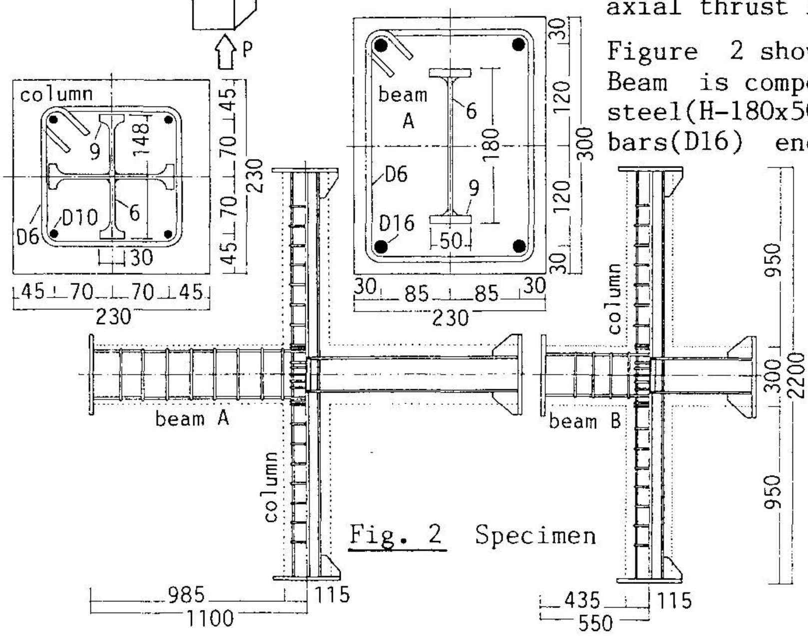

Fig. 2 Specimen

Figure 2 shows details of the specimen. Beam is composed of a built-up H-shaped steel(H-180x50x6x9) and 4 deformed bars(D16) encased in the rectangular concrete section of 230x300 mm, while column steel of a cross H-section formed by welding two rolled H-shaped steel(H-148x100x6x9), of which flange tips are cut off by the flame, is encased in the square concrete section of 230x230 mm with 4 of D10. Panels of the beam-to-column connection of the column-failing type specimens are strengthened by the doubler plates of 2-PL9.

Figure 3 shows the relations between the load Q and the relative displacement at the column end Δ against the beam A tip. Dashed line indicates the ultimate strength calculated by the SRC Standard of Architectural Institute of Japan.

3. CONCLUSIONS

1) Hysteresis loops of all specimens shows the pinched shape at first few cycles of loading, and then they gradually shift to the spindle shape.
2) Maximum strength of the P-series specimens subjected to bi-axial bending could not reach the calculated ultimate strength. Biaxial bending may affect on the strength of the connection panel.
3) Among the column-failing specimens, the deformation and energy dissipation capacities of C4000 are much larger than others, and C8031 shows rather brittle failure. The three-dimensional loading and bi-axial bending decrease the deformation and energy dissipation capacities.
4) The deformation and energy dissipation capacities of the panel-failing specimens are better than those of the column-failing specimens. The panel-failing type may be more advantageous than the column-failing type.
5) Two modes of the column deformation are observed: First, the symmetric doglegged configuration repeatedly appears in the positive and negative loadings, and the beam-to-column connection symmetrically moves back and forth on the horizontal line, as observed in C4000 and P-series specimens except P8031. Other specimens show the second mode, in which the doglegged configuration never recovers, once it occurs in one direction, and the horizontal movement of the connection accumulates in one direction. The former shows more stable behavior than the latter.

Table 1 Experimental Parameters

Specimen	P(kN)*	W1, W2(kN)	Failure type
C4000	392(20)	0, 0	Column
C4011	392(20)	9.8, 9.8	Column
C4031	392(20)	9.8, 29.4	Column
C8031	784(40)	9.8, 29.4	Column
P4000	392(15)	0, 0	Panel
P4011	392(15)	9.8, 9.8	Panel
P4031	392(15)	9.8, 29.4	Panel
P8031	784(30)	9.8, 29.4	Panel

*Constant axial thrust, and ratio to the squash load in parenthesis

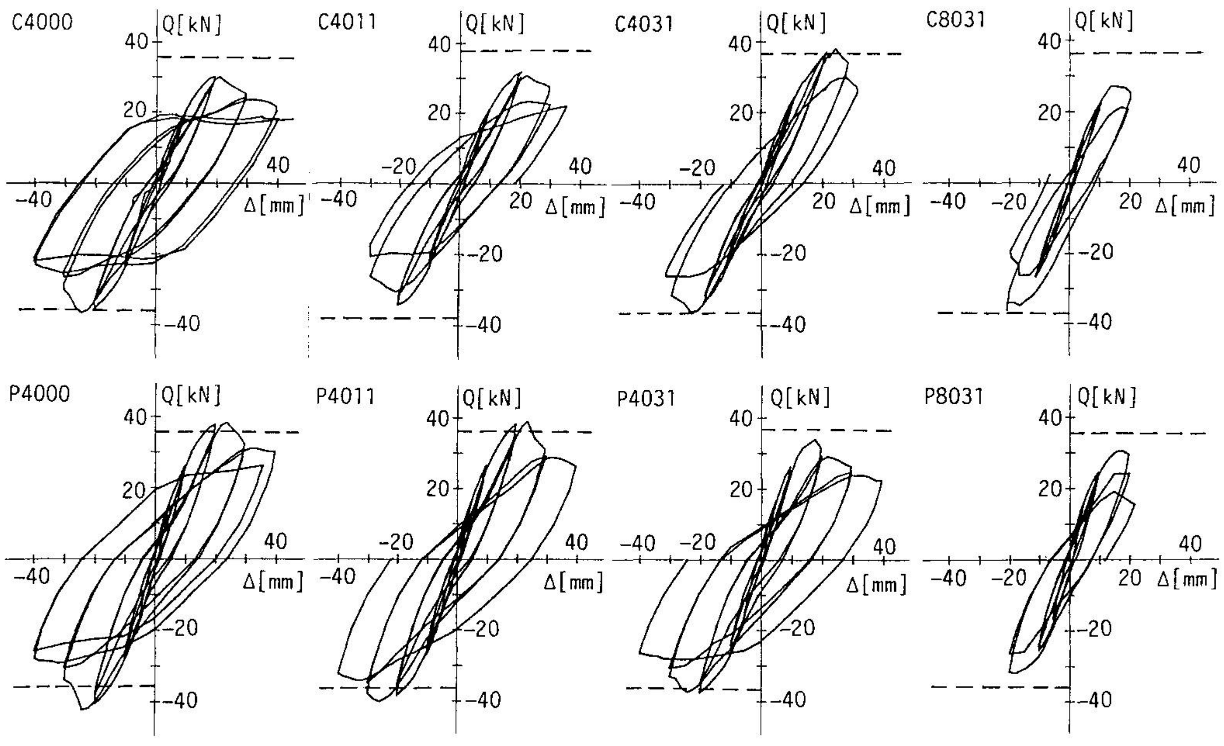

Fig. 3 Relations between Load Q and Displacement Δ